Supporting Information

Spontaneous and photomechanical twisting of a cyanostilbene-based molecular crystal

Pengyu Li, Jun Guan,* Min Peng, Junhong Wu, and Meizhen Yin*

Experimental Procedures

Materials:

All reagents were purchased from commercial sources and used without further purification. Solvents were purified according to standard laboratory methods. The reagents used for the synthesis were commercially available without further purification.

Structural characterizations:

The molecular structures were confirmed using ^{1}H NMR and high-resolution ESI mass spectroscopy. ^{1}H-NMR spectra were recorded on a Bruker 400 (400 MHz ^{1}H) spectrometer at room temperature.

Spectra measurements:

The UV-Vis absorption spectra were measured on a UV-2600 spectrometer. Fourier transform infrared (FTIR) spectra were obtained using a Thermo Nicolet Nexus FTIR device with a Smart Golden Gate ATR attachment in the range of 4000–500 cm^{-1} with 2 cm^{-1} resolution. The micro-Raman spectra were collected using a confocal Raman microscope (Horiba LabRAM HR Evolution , Japan), equipped with a CCD detector and excited using a 785 nm Omnichrome Argon ion laser.

Powder X-ray diffraction:

X-ray diffraction (XRD) patterns of the powder were recorded using a Rigaku 2500VB2+PC diffractometer using the Cu Kα radiation (λ=1.541844 Å) at 40 kV and 50 mA with the step-scanned mode in 0.04° (2θ) per step and count time of 10s/step in the range from 5 to 40°.

Single-crystal X-ray diffraction:

Single crystal X-ray diffraction measurements were carried out on a Bruker D8 Venture diffractometer outfitted with a PHOTON-100 CMOS detector, using monochromatic microfocus MoKα radiation (λ = 0.71073 Å) that was operated at 50 kV and 40 mA at 153 K by chilled nitrogen flow controlled by a KRYOFLEX II low temperature attachment. Single crystals were selected and mounted on a nylon loop in Paratone-N cryoprotectant. Unit cell determination was performed in the Bruker SMART APEX III software suite. The data sets were reduced and a multi-scan spherical absorption correction was implemented in the SCALE interface and refined with the Shelx2014 software package.

Theoretical calculations:

DFT simulations: The DFT simulations were carried out with the Gaussian 09 package[S1]. The B3LYP functional and the 6-31G basis set was applied, since it represents a good balance between quality of the results and computational cost. **Crystal structure calculations:** The crystal structure of *d*-CS-H is constructed from CS-H crystal. This crystal structure was optimized by DFT-D calculations (PBE exchange-correlation function with Grimme-06 semiempirical dispersion correction54) using CASTEP in Material Studio software package [S2]. In the calculations, all atom positions and cell parameters were optimized (1200 eV cutoff level). To compare the structural changes in detail, the crystal structure of CS-H was also optimized, starting from the observed crystal structure, using the same method as for the crystal after photoreactions. **Intermolecular interaction analysis:** The interaction energy frameworks for CS-H and CS-O crystals are calculated by using CrystalExplorer 17.5 [S3].

Synthesis and characterizations
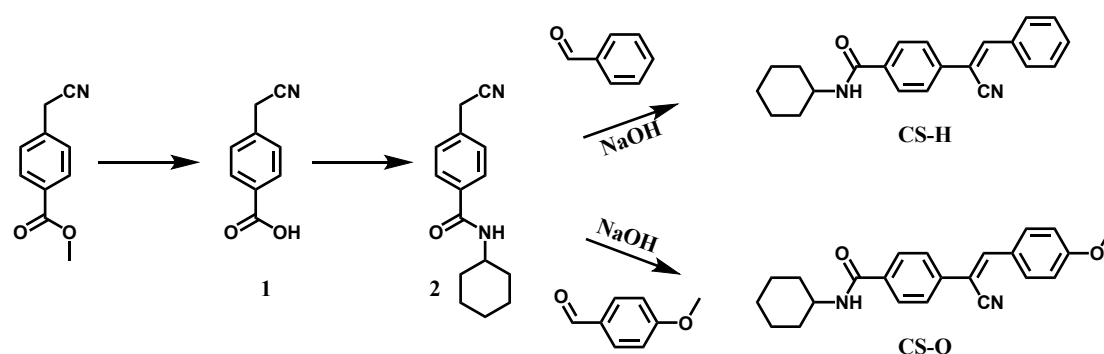
Scheme S1. Synthesis routes of compounds CS-H and CS-O.

4-(cyanomethyl)benzoic acid (1):

The methyl 4-(cyanomethyl)benzoate (1.75 g, 10 mmol) was dissolved into 50 mL of the mixture of THF/ethanol/water with 1:1:1 ratio. After adding 400 mg NaOH, the obtained suspension is heated and reflux at 80 °C for 8 h. The reaction progress was monitored by TLC chromatographic method. After cooling to room temperature, the reaction mixture was poured into 250 mL deionized water with continually stirring. Then hydrochloric acid solution was added to acidify the mixture upon to pH = 1.0 and afford the yellowish precipitate. The product was collected by vacuum suction filter and washed by 50 mL water for 3 times to give light yellow solid. The obtained filter cake was dried for further synthesis.

4-(cyanomethyl)-N-cyclohexylbenzamide (2):

A mixture of 1 (800 mg, 5.0 mmol), 1-ethyl-3-(3-dimethylaminopropyl) carbodiimide hydrochloride (EDC·HCl, 958.5 mg, 5.0 mmol), 1-hydroxybenzotrizole (HOBt, 524 mg, 4 mmol) and *N, N*-Diisopropylethylamine (DIPEA, 646 mg, 5.0 mmol) in dichloromethane (DCM, 35 ml) was stirred at room temperature for 30-40 min. Cyclohexanamine (500 mg, 5 mmol) was dissolved in 5 mL DCM and added into the reaction mixture. After stirring for 48 h at room temperature, the reaction mixture was concentrated under reduced pressure. The residue was washed by 5 mL iced ethanol for 3 times and purified by column chromatography (DCM: Methanol = 200:1) to give a white solid 836 mg (yield: 69%).

(Z)-4-(1-cyano-2-phenylvinyl)-*N*-cyclohexylbenzamide (CS-H):

A mixture of 2 (120 mg, 0.5 mmol) and benzaldehyde (150 mg, ~0.75 mmol) in ethanol solution is added with 20 mg NaOH and continuously stirred at room temperature. After stirring for about 30 s, white precipitates would be obtained. After stirring for 1.0 h, the product was collected by vacuum suction filter and washed by 5 mL for 3 times to give white filter cake 130 mg (yield 78.8%). ^{1}H NMR (400 MHz, DMSO-d_6) δ 8.31 (d, J = 7.9 Hz, 1H), 8.17 (s, 1H), 7.97 (d, J = 7.9 Hz, 4H), 7.85 (d, J = 8.2 Hz, 2H), 7.55 (q, J = 8.5, 7.5 Hz, 3H), 3.86 – 3.69 (m, 1H), 1.84 (m, 2H), 1.78 – 1.67 (m, 2H), 1.62 (m, 1H), 1.34 (m, 4H), 1.15 (m, 1H). ^{13}C NMR (101 MHz, DMSO) δ 164.94, 144.49, 136.45, 135.68, 134.06, 131.37, 129.76, 129.48, 128.60, 126.00, 118.18, 110.13, 48.94, 32.88, 25.74, 25.43.

(Z)-4-(1-cyano-2-(4-methoxyphenyl)vinyl)-N-cyclohexylbenzamide (CS-O):

A mixture of 2 (120 mg, 0.5 mmol) and 4-methoxybenzaldehyde (150 mg, ~0.75 mmol) in ethanol solution is added with 20 mg NaOH and continuously stirred at room temperature. After stirring for about 30 s, yellowish precipitates would be obtained. After stirring for 1.0 h, the product was collected by vacuum suction filter and washed by 5 mL for 3 times to give white yellow cake 153 mg (yield 85.0%). ^{1}H NMR (400 MHz, DMSO-d_6) δ 8.30 (d, J = 7.9 Hz, 1H), 8.09 (s, 1H), 7.99 (d, J = 8.9 Hz, 2H), 7.95 (d, J = 8.6 Hz, 2H), 7.80 (d, J = 8.5 Hz, 2H), 7.13 (d, J = 8.9 Hz, 2H), 3.85 (s, 3H), 3.82 – 3.71 (m, 1H), 1.83 (m, 2H), 1.79 – 1.68 (m, 2H), 1.60 (m, 1H), 1.32 (m, 4H), 1.19 – 1.06 (m, 1H). ^{13}C NMR (101 MHz, DMSO-d_6) δ 144.03, 136.90, 135.18, 131.87, 128.57, 126.58, 125.63, 118.71, 115.04, 106.75, 55.97, 48.92, 32.89, 25.75, 25.44.
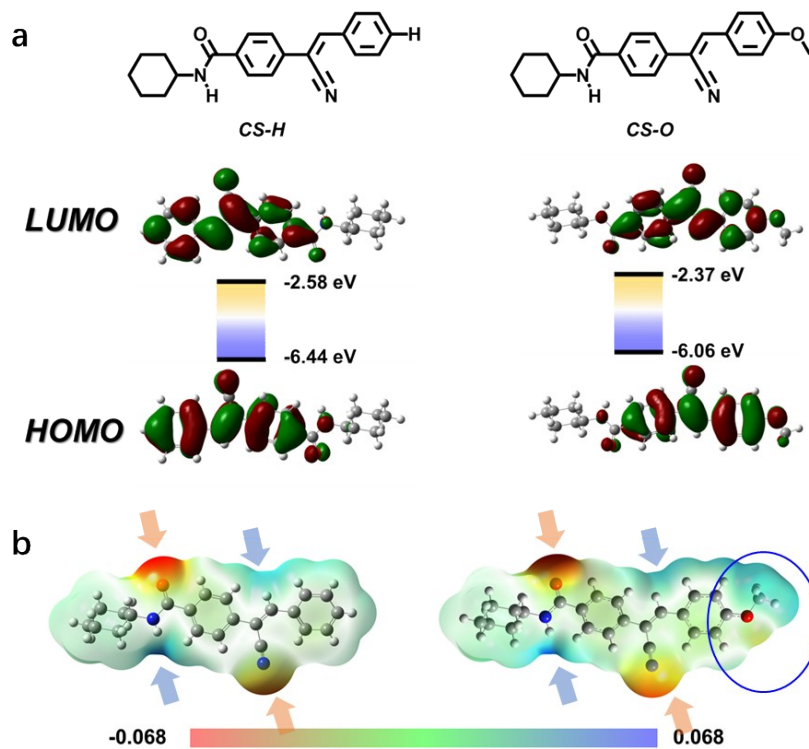
Figure S1. (a) Density-function theory (DFT) calculated highest occupied molecular orbitals (HOMOs) and lowest unoccupied molecular orbitals (LUMOs), and Time-dependent DFT (TD-DFT) calculated absorbance spectra of CS-H And CS-O, respectively, in gas states (isovalue = 0.02). (b) Electrostatic potential surface of CS-H and CS-O.
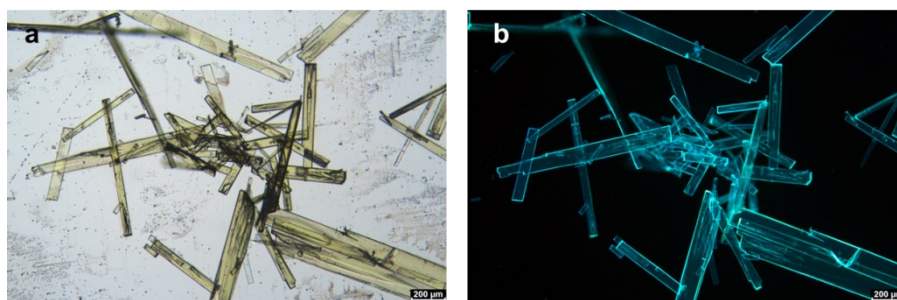
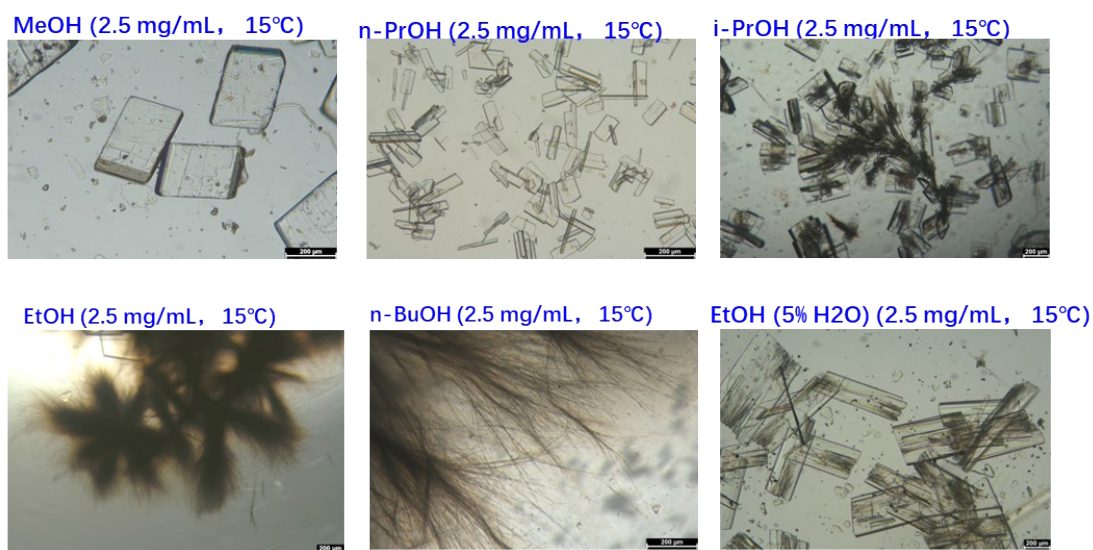**Figure S2.** Photographs of CS-O crystals under (a) room light and (b) UV light.

MeOH (2.5 mg/mL，15℃)　　n-PrOH (2.5 mg/mL，15℃)　　i-PrOH (2.5 mg/mL，15℃)

EtOH (2.5 mg/mL，15℃)　　n-BuOH (2.5 mg/mL，15℃)　　EtOH (5% H2O) (2.5 mg/mL，15℃)

Figure S3. Solvent-dependent crystal morphology of CS-H.

EtOH (2.5 mg/mL，4℃)　　BuOH (2.5 mg/mL，4℃)　　BuOH (2.5 mg/mL，4℃, POM image)

EtOH (2.5 mg/mL，30℃)　　BuOH (2.5 mg/mL，30℃)　　BuOH (2.5 mg/mL，30℃, POM image)
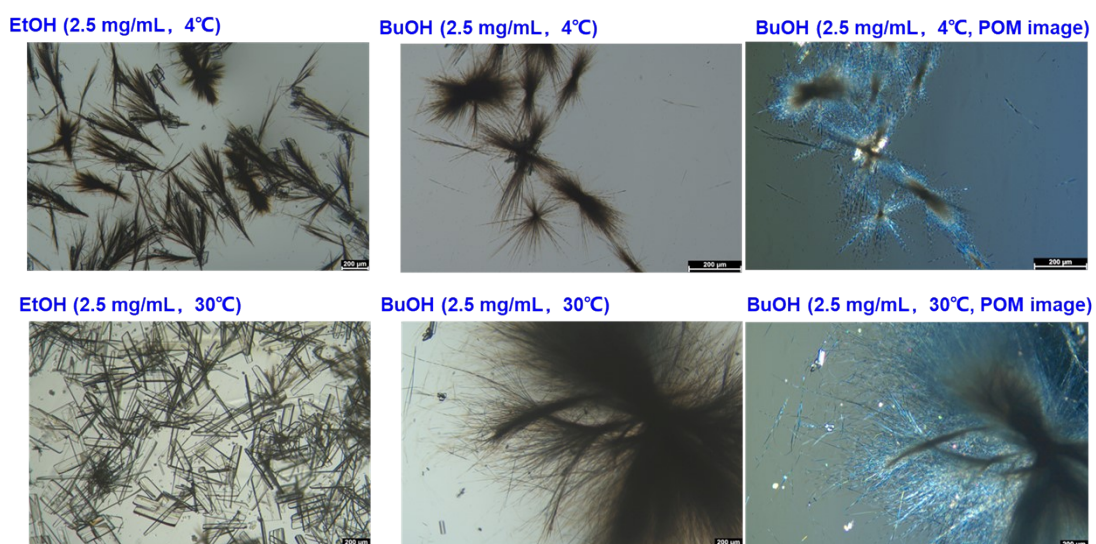
Figure S4. Temperature-dependent crystal morphology of CS-H.

Table S1. Summarization of CS-H

	Solvent	Concentration (mg/mL)	Temperature (°C)	Morphology	Features
Solvent-dependent	Methanol	2.5	15	Microblock	
	Ethanol	2.5	15	Microtwist + Microblock	
	Ethanol + 2% H2O	2.5	15	microblock	
	Propanol	2.5	15	Microblock	
	Isopropanol	2.5	15	Microblock	
	n-Butanol	2.5	15	Microtwist + Microblock	
Concentration-dependent	Ethanol	5	15	Microtwist + Microblock	Heterojunction
	n-Butanol	5	15	Microblock	crystal particle
Temperature-dependent	Ethanol	2.5	4	Microtwist + Microblock	Heterojunction
	Butanol	2.5	4	Microtwist	Shortened pitch
	Ethanol	2.5	30	Microblock	
	Butanol	2.5	30	Microtwist + Microblock	Elongated pitch
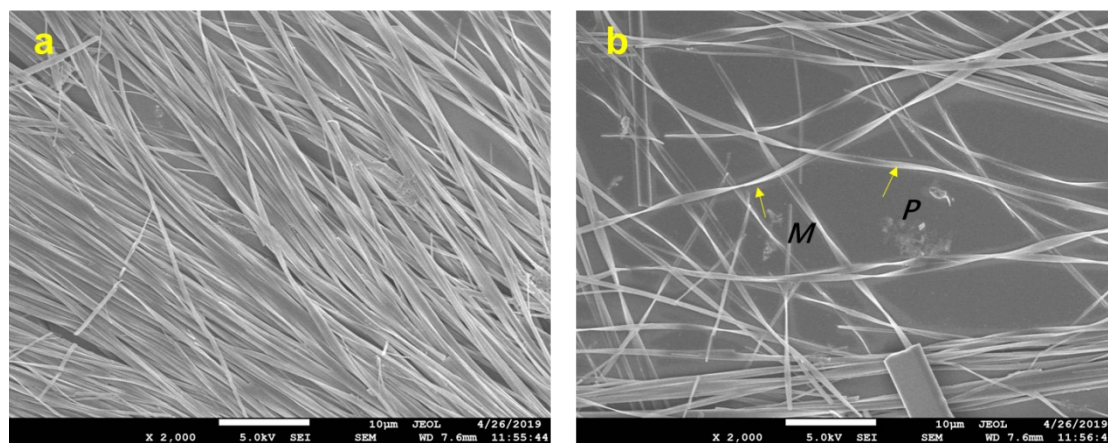
Figure S5. SEM images of CS-H microtwists.
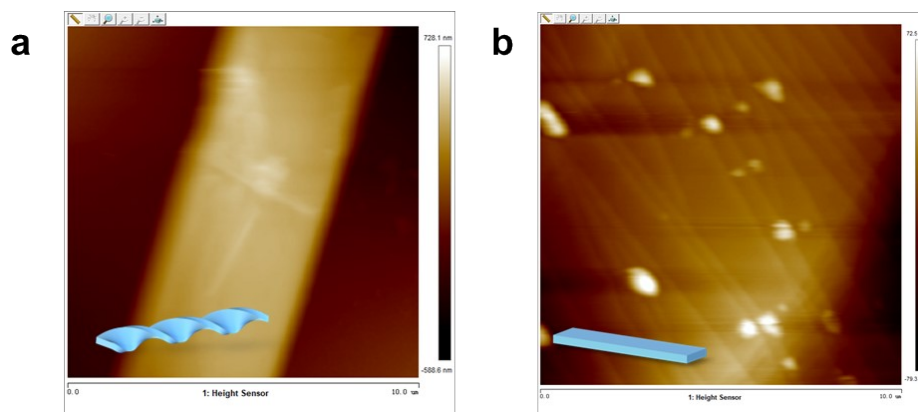
Figure S6. AFM images of CS-H microtwist and surface morphology of CS-H microplate.
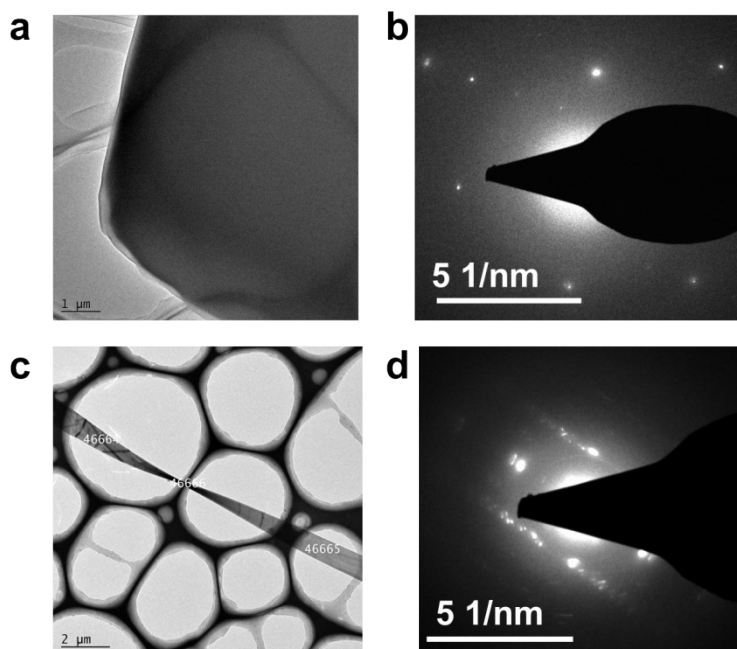
Figure S7. TEM images of a CS-H (a) microplate and (c)microhelix. The SAED pattern of the relevant (b) microplate and (d)microhelix.
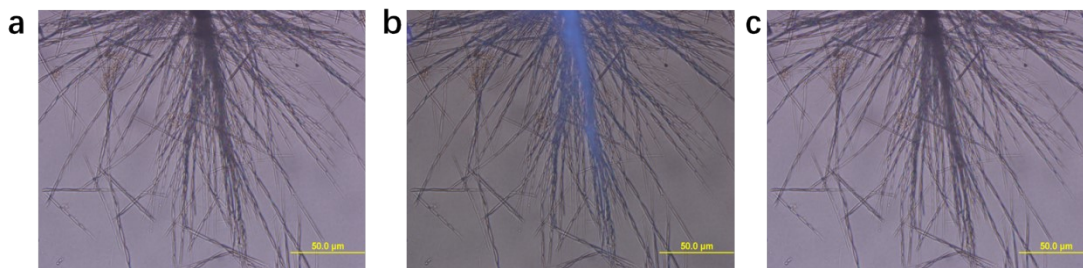
Figure S8. Photoresponses of the microhelices under UV irradiation. (a) pristine state, (b) being UV irradiation and (c) after UV irradiation.
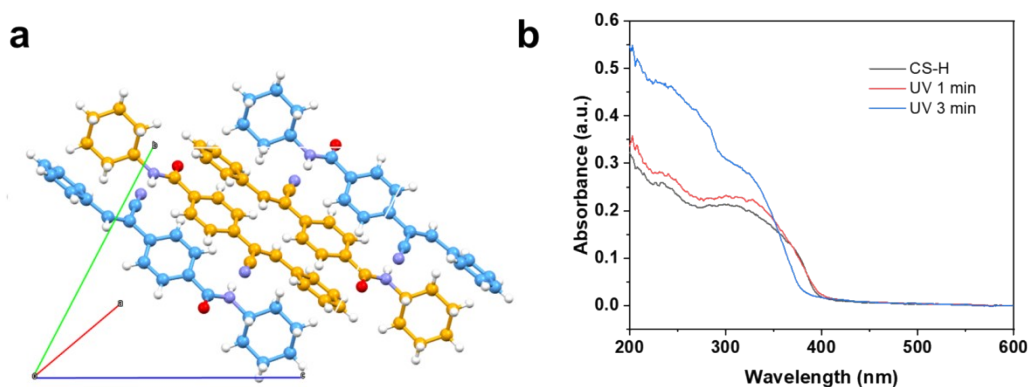

Figure S9. (a) The lattice structure of CS-H crystal and the pai-dimer suitable for [2+2] cycloaddition that is labelled by yellow color. (b) Change of absorbance spectra of CS-H crystals under UV light irradiation for different time.
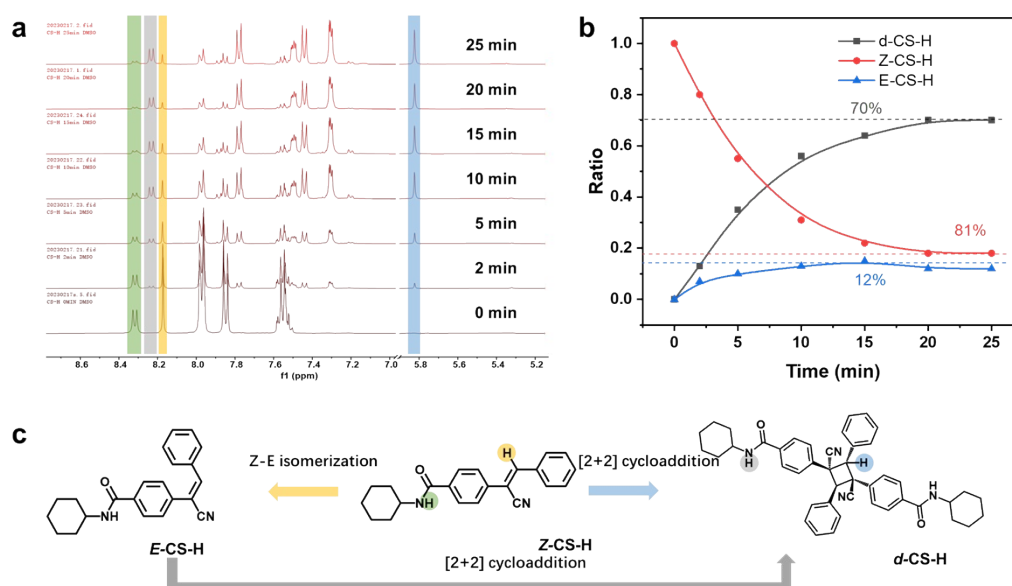
Figure S10. (a) Time-dependent ^{1}H NMR spectra of CS-H crystal before and after UV irradiation for 20 min. (b) The yield of photoreaction and conversion as a function of time. (c) illustrations of the photoreactions in CS-H crystal.
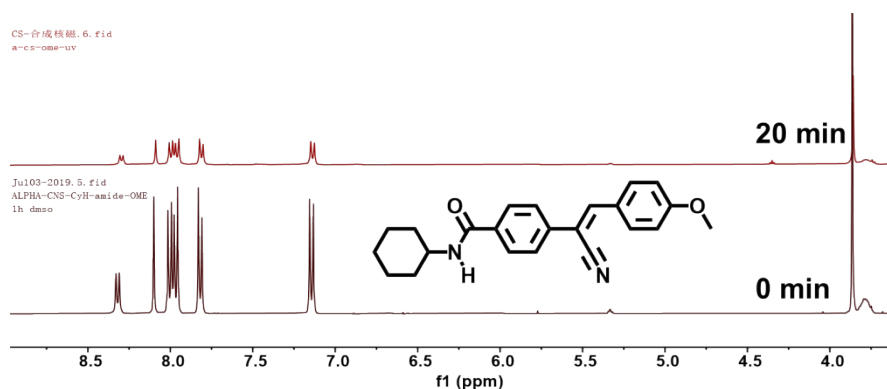
Figure S11. ^{1}H NMR spectra of CS-H crystal before and after UV irradiation for 20 min.

Table S2. Crystal data and structure refinement for CS-H and CS-O.

Compound	CS-H	CS-O
CCDC number	2225644	2225645
Empirical formula	$C_{22}H_{22}N_2O$	$C_{23}H_{24}N_2O_2$
Formula weight	330.42	360.44
Temperature / K	297.0(6)	117(3)
Crystal system	triclinic	triclinic
Space group	*P*-1	*P*-1
a / Å	11.9988(15)	6.4239(6)
b / Å	13.484(2)	11.8514(12)
c / Å	13.898(2)	12.7044(11)
α/°	61.836(18),	81.949(8)
β/°	74.537(13),	82.716(7)
γ/°	70.969(14)	87.297(8)
Volume / Å3	1856.8(5)	949.53(15)
Z	4	2
ρcalc / mg mm-3	1.182	1.261
μ / mm-1	0.073	0.081
F(000)	704	384
Crystal size / mm3	0.33 × 0.27 × 0.11	0.56 × 0.47 × 0.07
2Θ range for data collection	6.02 to 52°	6.52 to 52°
Index ranges	-14 ≤ h ≤ 14 -16 ≤ k ≤ 16 -17 ≤ l ≤ 15	-7 ≤ h ≤ 7 -14 ≤ k ≤ 14 -15 ≤ l ≤ 15
Reflections collected	14664	6268
Independent reflections	7132[R(int) = 0.0797 (inf-0.9Å)]	3635[R(int) = 0.0376 (inf-0.9Å)]
Data/restraints/parameters	7132/0/452	3635/0/245
Goodness-of-fit on F2	0.970	1.039
Final R indexes [I>2σ (I) i.e. Fo>4σ (Fo)]	R1 = 0.0765, wR2 = 0.1502	R1 = 0.0559, wR2 = 0.1169
Final R indexes [all data]	R1 = 0.2668, wR2 = 0.2503	R1 = 0.0852, wR2 = 0.1407
Largest diff. peak/hole / e Å-3	0.215/-0.171	0.202/-0.262
Flack Parameters	N	N
Completeness	0.9982	0.9982

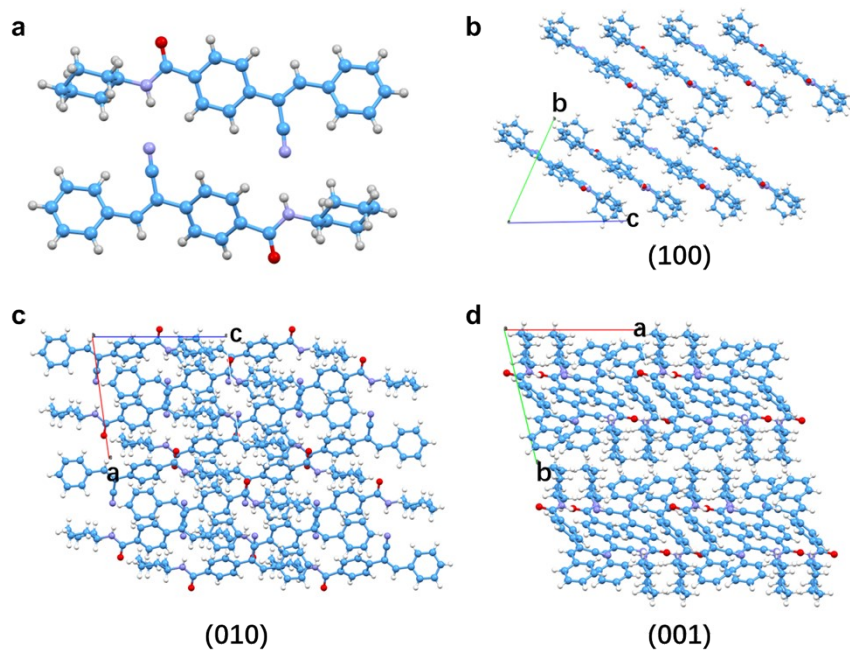**Figure S12.** (a) Crystal structure of CS-H. Viewing from (b) (100) face, (c) (010) face and (d) (001) face of a 2×2×2 superlattice.
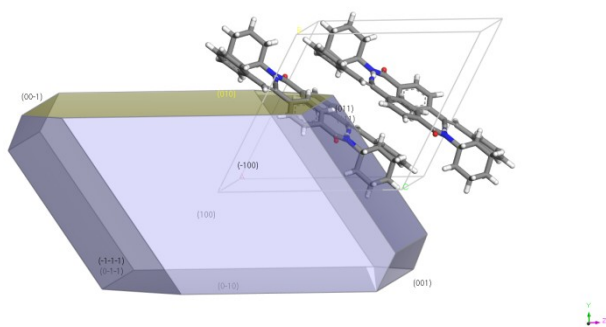

Figure S13. The growth morphology of CS-H crystal simulated by Materials Studio software.

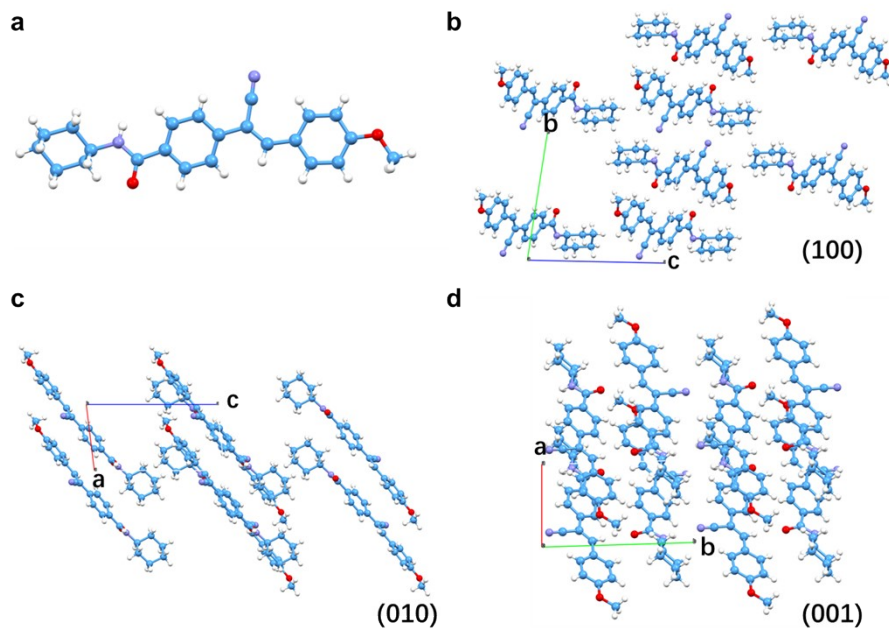**Figure S14.** (a) Crystal structure of CS-O. Viewing from (b) (100) face, (c) (010) face and (d) (001) face of a 2×2×2 superlattice.
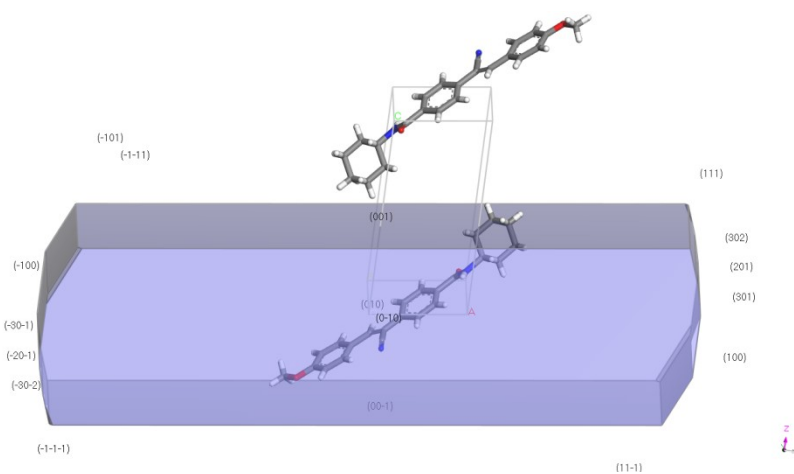

Figure S15. The growth morphology of CS-O crystal simulated by Materials Studio software.
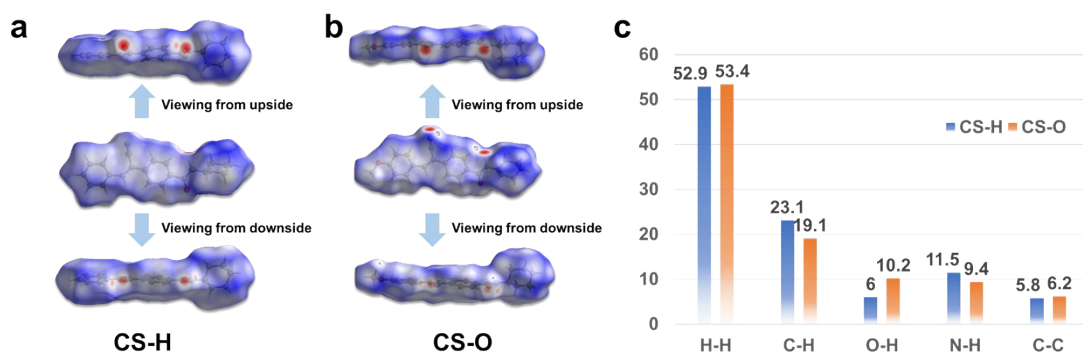
Figure S16. (a) Hirshfeld surfaces of CS-H and CS-O viewing from different directions. (b) Histogram of the intermolecular interactions.
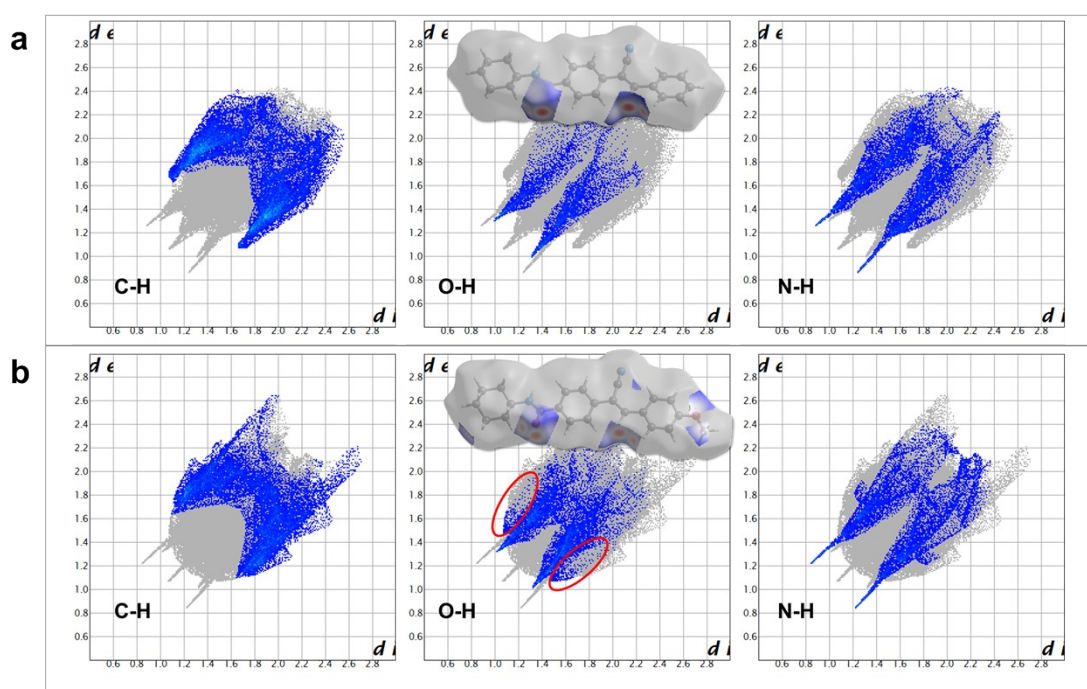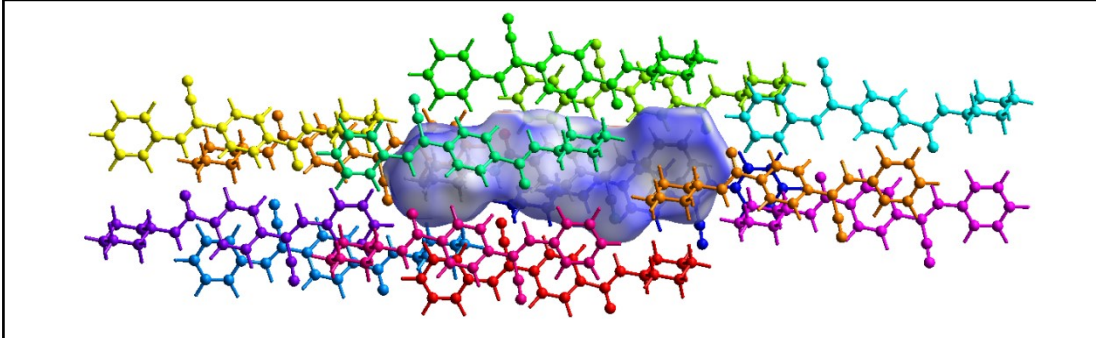

Figure S17. 2D fingerprint plots of C-H, O-H and N-H interactions in (a) CS-H crystal and (b) CS-O crystal.

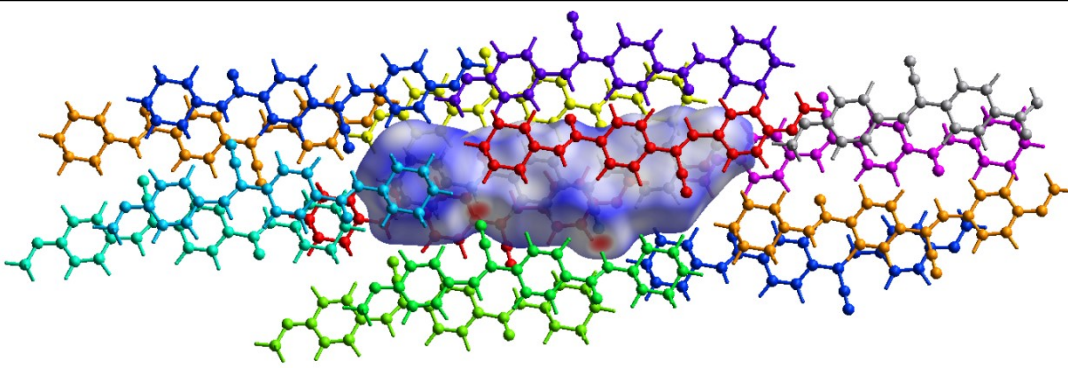**Table S3.** Interaction energies in CS-H crystal.

Interaction Energies (kJ/mol); R is the distance between molecular centroids (mean atomic position) in Å; Total energies, only reported for two benchmarked energy models, are the sum of the four energy components, scaled appropriately (see the scale factor table below)

	N	Symop	R	Electron Density	E_ele	E_pol	E_dis	E_rep	E_tot
	1	-	6.10	B3LYP/6-31G(d,p)	-57.7	-16.3	-39.3	66.0	-66.5
	0	x, y, z	14.07	B3LYP/6-31G(d,p)	-4.2	-0.4	-20.2	12.1	-14.8
	0	-x, -y, -z	8.33	B3LYP/6-31G(d,p)	-1.6	-1.9	-22.4	9.1	-17.0
	0	-	19.17	B3LYP/6-31G(d,p)	-1.1	-0.3	-9.0	8.0	-4.3
	0	-x, -y, -z	19.00	B3LYP/6-31G(d,p)	-0.5	-0.3	-5.2	1.5	-4.4
	0	-	6.80	B3LYP/6-31G(d,p)	-10.5	-2.4	-64.4	27.9	-51.7
	0	-x, -y, -z	18.97	B3LYP/6-31G(d,p)	-0.6	-0.0	-9.3	4.4	-6.1
	0	-	5.93	B3LYP/6-31G(d,p)	-39.3	-13.6	-48.5	53.7	-60.6
	0	-	14.78	B3LYP/6-31G(d,p)	0.4	-0.2	-5.4	0.5	-4.1
	0	-x, -y, -z	6.77	B3LYP/6-31G(d,p)	-10.5	-1.4	-74.3	35.1	-55.2
	1	-	18.80	B3LYP/6-31G(d,p)	-0.7	-0.2	-7.1	2.9	-5.3

Table S4. Interaction energies in CS-O crystal.

Interaction Energies (kJ/mol); R is the distance between molecular centroids (mean atomic position) in Å; Total energies, only reported for two benchmarked energy models, are the sum of the four energy components, scaled appropriately (see the scale factor table below)

|	N	Symop	R	Electron Density	E_ele	E_pol	E_dis	E_rep	E_tot
	1	x, y, z	6.42	B3LYP/6-31G(d,p)	-13.6	-3.5	-95.9	55.7	-66.0
	1	x, y, z	19.18	B3LYP/6-31G(d,p)	-1.9	-0.4	-9.6	4.6	-7.9
	0	-x, -y, -z	5.79	B3LYP/6-31G(d,p)	-36.6	-14.8	-52.4	53.3	-62.3
	0	-x, -y, -z	9.84	B3LYP/6-31G(d,p)	-1.9	-2.6	-14.6	5.7	-13.2
	1	-x, -y, -z	6.41	B3LYP/6-31G(d,p)	-58.6	-16.2	-43.2	76.8	-64.2
	0	-x, -y, -z	20.67	B3LYP/6-31G(d,p)	-0.5	-0.0	-8.9	3.4	-6.2
	1	-x, -y, -z	16.38	B3LYP/6-31G(d,p)	-0.5	-0.2	-10.3	4.0	-7.1
	1	x, y, z	14.95	B3LYP/6-31G(d,p)	-1.8	-0.3	-11.0	4.8	-8.6
	1	-x, -y, -z	7.29	B3LYP/6-31G(d,p)	-17.1	-6.5	-48.1	35.6	-42.7
	0	-x, -y, -z	18.07	B3LYP/6-31G(d,p)	-8.8	-1.5	-20.7	15.7	-18.8
	1	-x, -y, -z	23.06	B3LYP/6-31G(d,p)	1.6	-0.7	-3.6	3.9	0.5
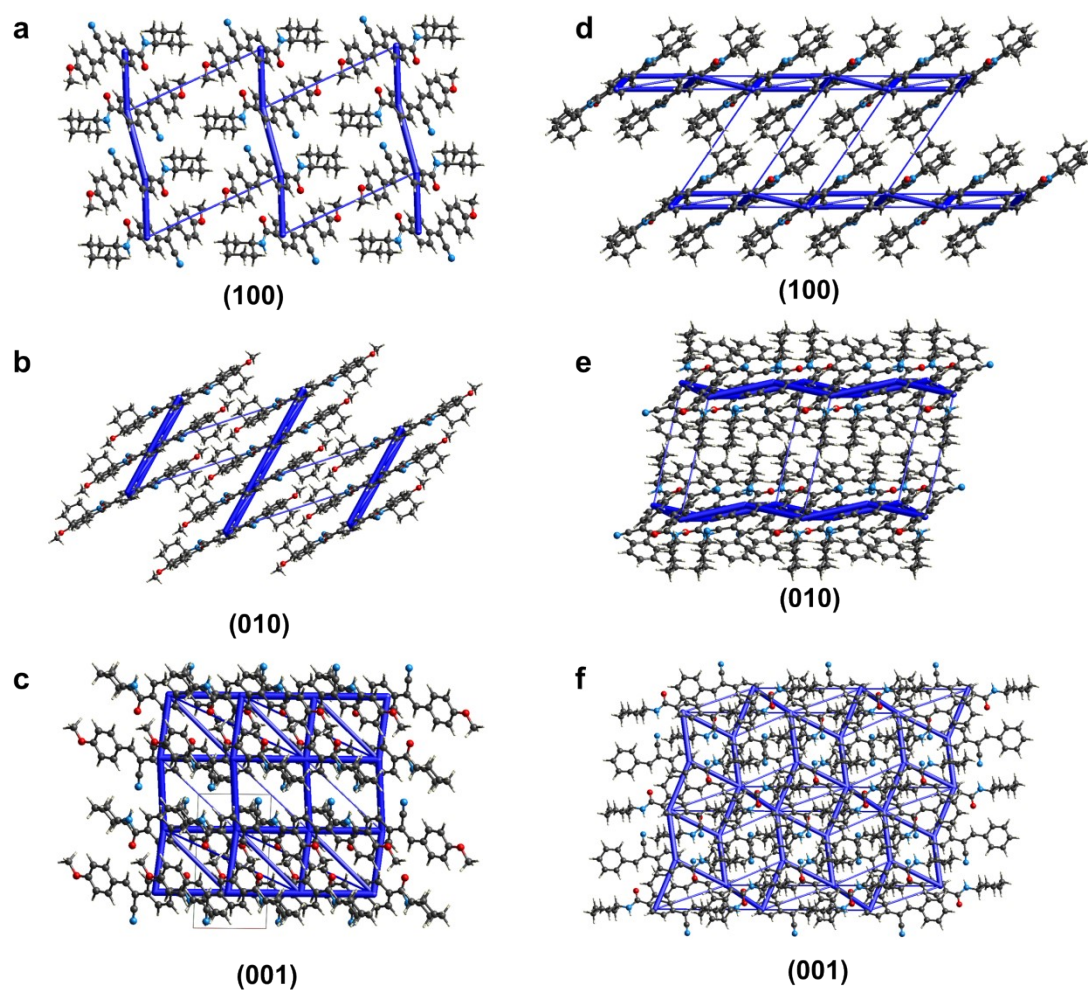
Figure S18. Energy frameworks of (a-c) CS-O and (d-f) CS-H crystal viewing from (a) (100) face, (b) (010) face, and (c) (001) face.
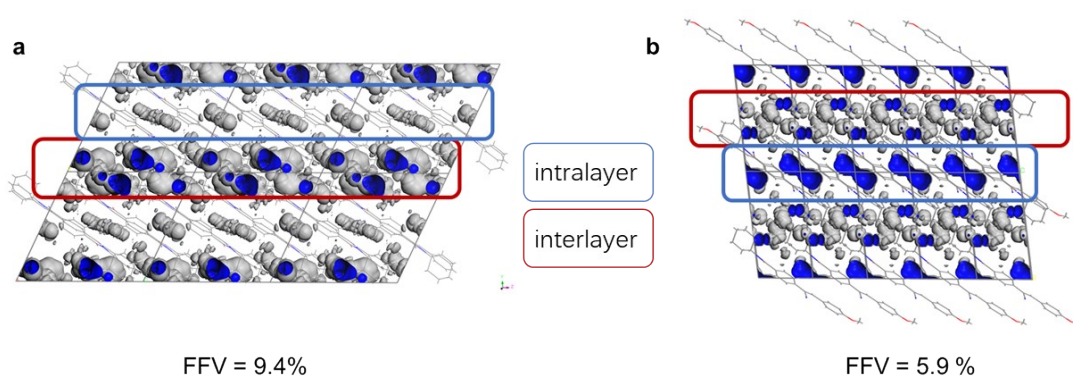

Figure S19. Distributions of free volume in (a) CS-H crystal and (b) CS-O crystal with their relative FFV value.
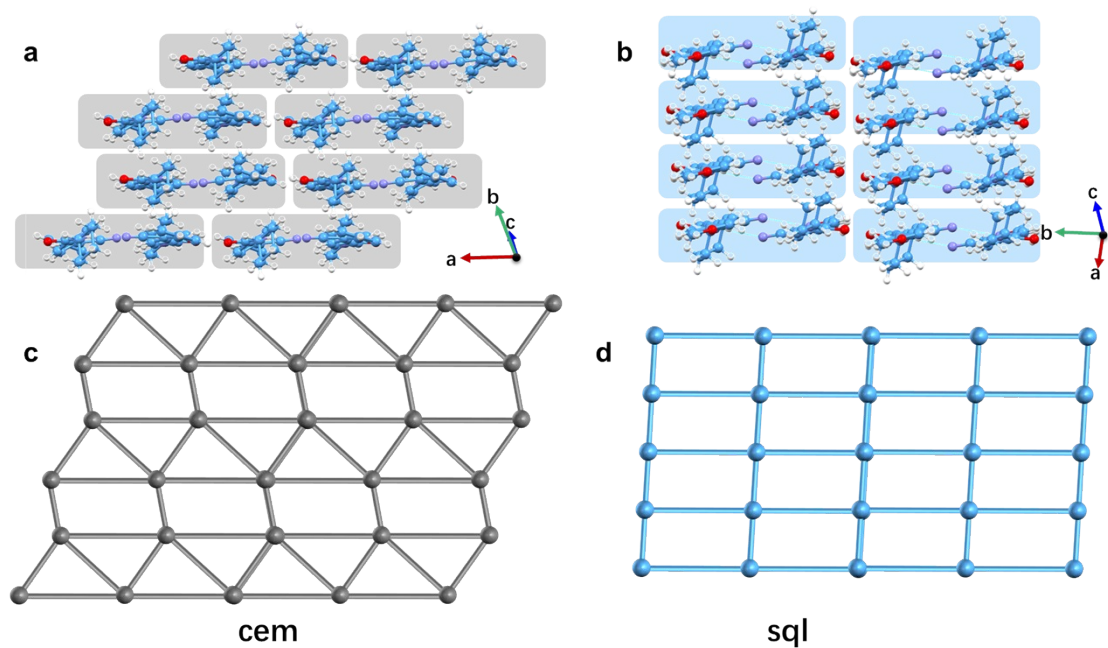
Figure S20. Molecular stacking within molecular layers in (a) CS-H crystal and (b) CS-O crystal. The simplified supramolecular topological networks of intralayer molecular stacking in (c) CS-H crystal and (d) CS-O crystal.
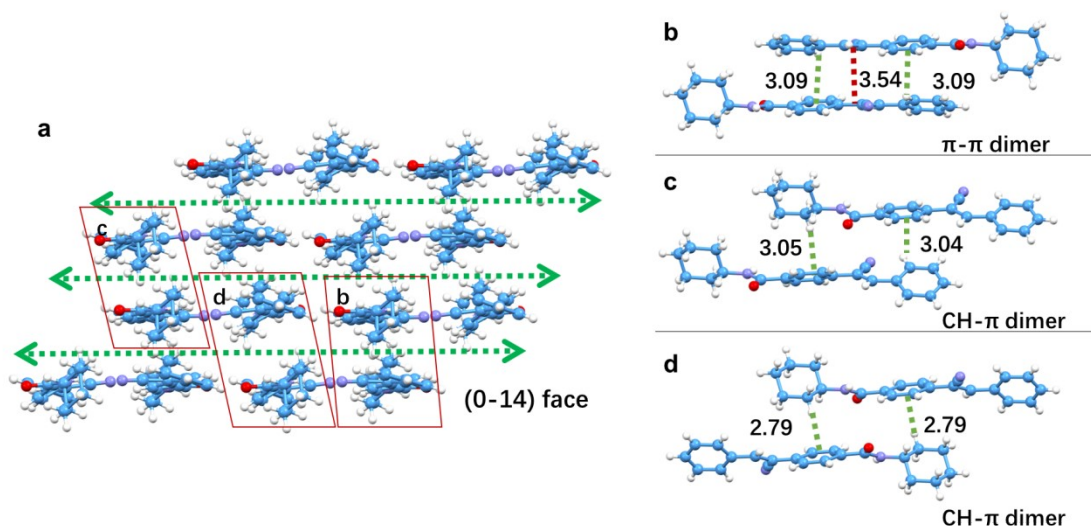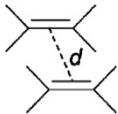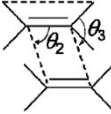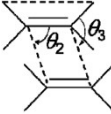

Figure S21. Molecular dimers in CS-H crystal.

Table S5. Geometric parameters among two adjacent C=C bonds for [2+2] cycloaddition reactions.

	d (Å)	θ_1 (°)	θ_2 (°)	θ_3 (°)
ideal	< 4.2	0	90	90
CS-H	3.96	0	62.87	83.29
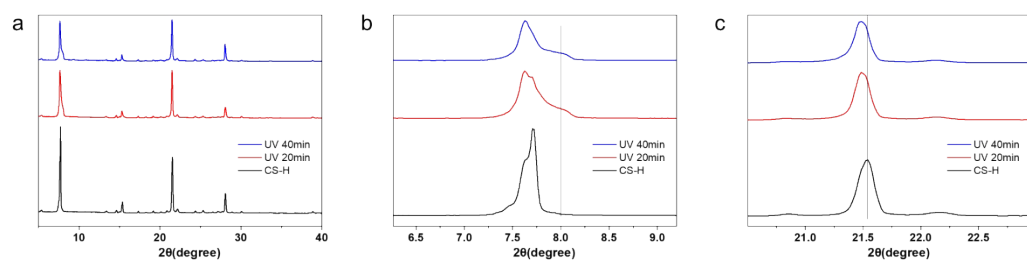
Figure S22. Changes of the PXRD patterns of CS-H crystal under UV irradiation for different time.

8.32
8.30
8.17
7.98
7.96
7.86
7.84
7.58
7.56
7.54
7.52
7.51

3.78
3.78
3.77
3.74
3.73

2.50 DMSO-d6

1.85
1.83
1.75
1.74
1.63
1.60
1.35
1.32
1.29
1.15

8.32
8.30
8.17
7.98
7.96
7.86
7.84
7.58
7.56
7.54
7.52
7.51

0.9
1.0
3.9
2.0
2.9

8.5 8.4 8.3 8.2 8.1 8.0 7.9 7.8 7.7 7.6 7.5 7.4
f1 (ppm)

0.9
1.0
3.9
2.0
2.9

1.0

2.0
1.9
1.0
4.0
1.0

14   13   12   11   10   9   8   7   6   5   4   3   2   1   0
f1 (ppm)
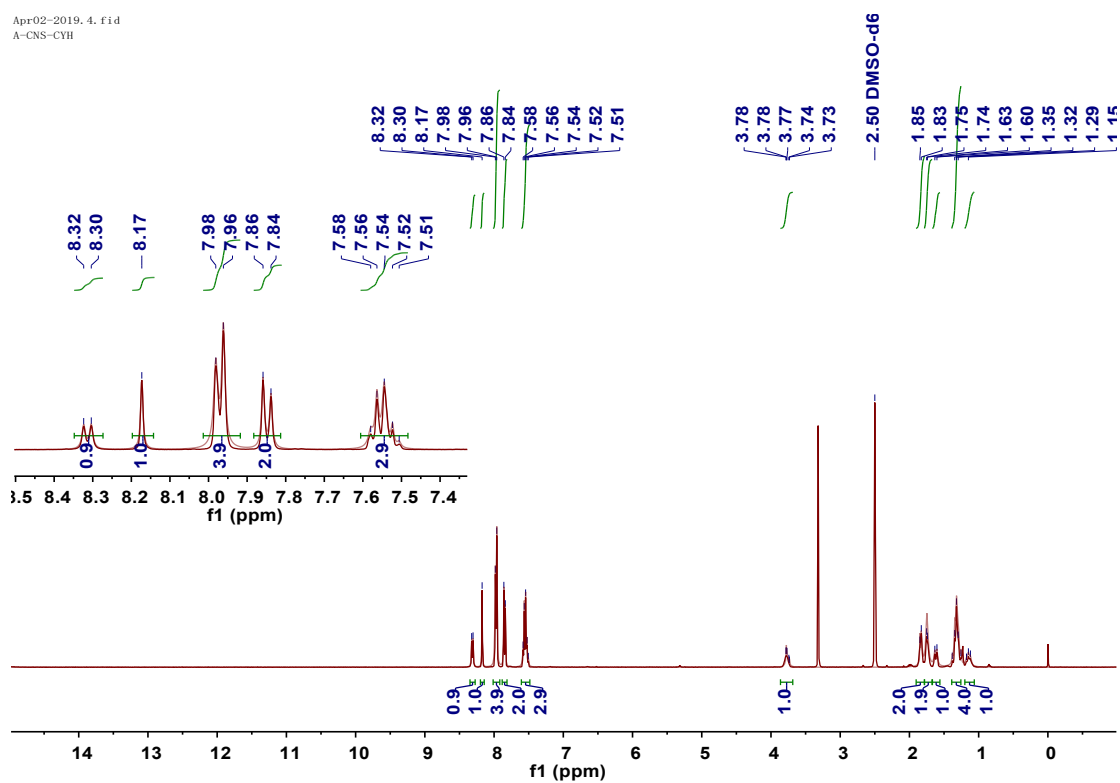
Figure S23. ^{1}H NMR spectrum of CS-H in DMSO-d_6.

164.94

144.49
136.45
135.68
134.06
131.37
129.76
129.48
128.60
126.00
118.18

110.13

48.94

32.88
25.74
25.43

80   170   160   150   140   130   120   110   100   90   80   70   60   50   40   30   2
f1 (ppm)
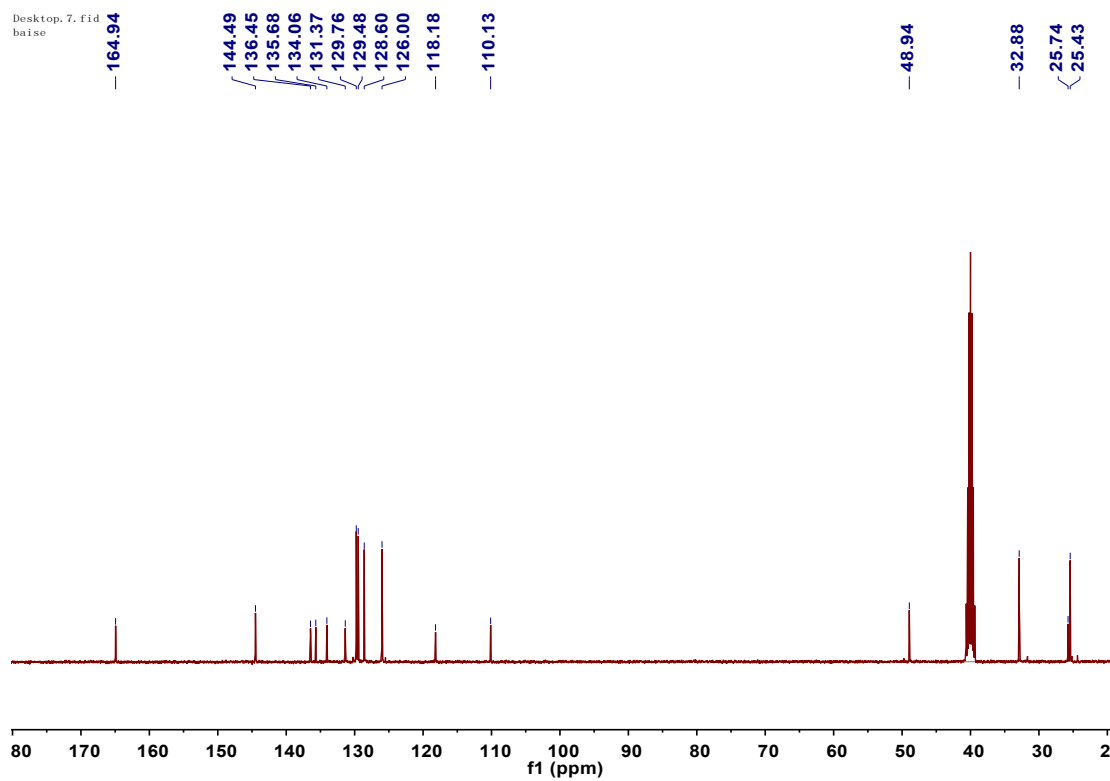
Figure S24. ^{13}C NMR spectrum of CS-H in DMSO-d_6..
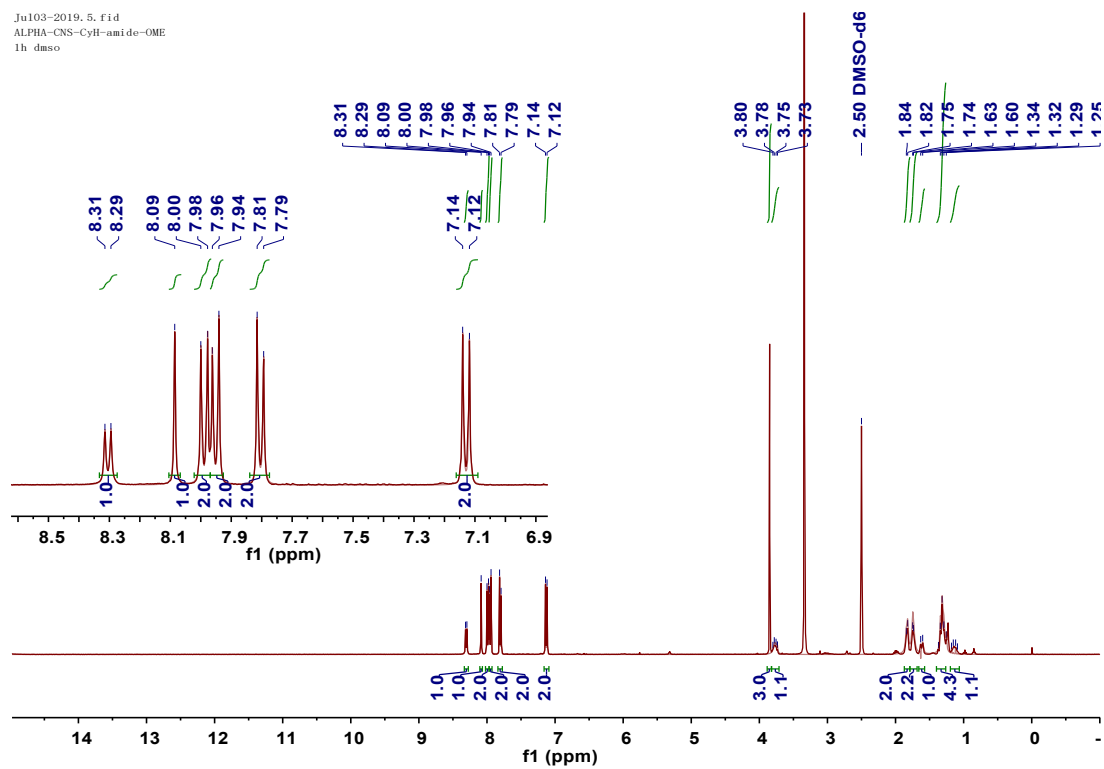
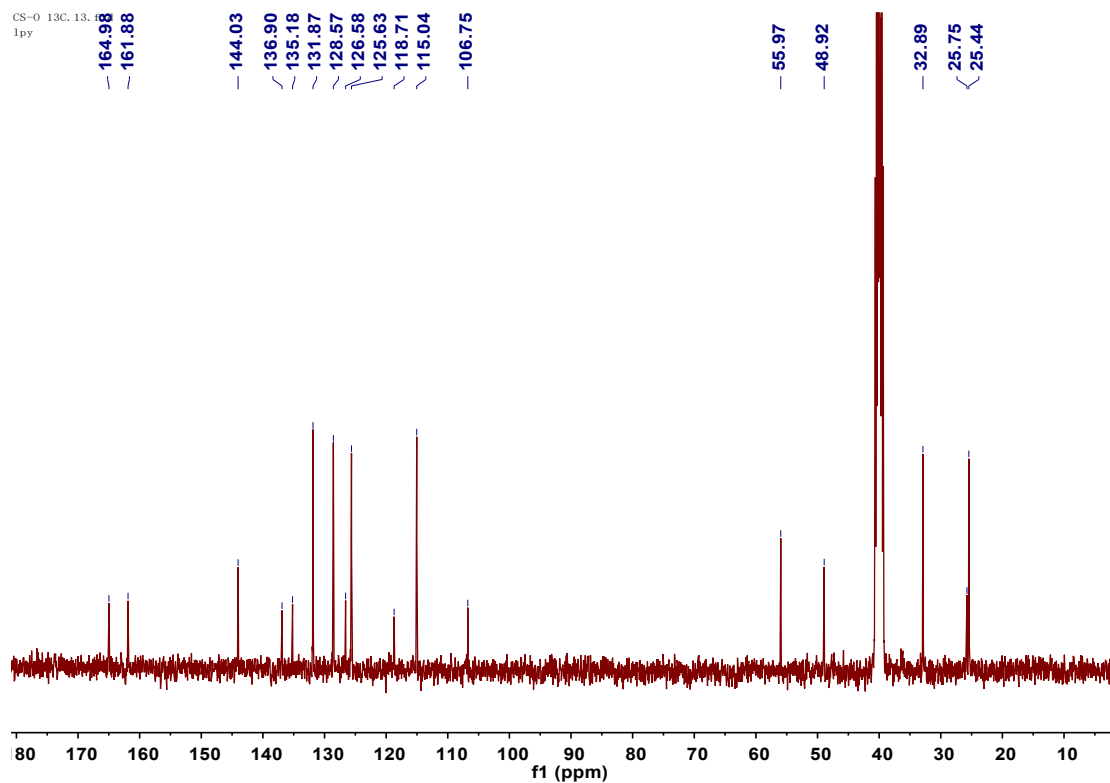**Figure S25.** ^{1}H NMR spectrum of CS-O in DMSO-d$_6$..

Figure S26. ^{13}C NMR spectrum of CS-O in DMSO-d$_6$.

References:

[S1] Gaussian 09, Revision D.01, M. J. Frisch, G. W. Trucks, H. B. Schlegel, G. E. Scuseria, M. A. Robb, J. R. Cheeseman, G. Scalmani, V. Barone, B. Mennucci, G. A. Petersson, H. Nakatsuji, M. Caricato, X. Li, H. P. Hratchian, A. F. Izmaylov, J. Bloino, G. Zheng, J. L. Sonnenberg, M. Hada, M. Ehara, K. Toyota, R. Fukuda, J. Hasegawa, M. Ishida, T. Nakajima, Y. Honda, O. Kitao, H. Nakai, T. Vreven, J. A. Montgomery, Jr., J. E. Peralta, F. Ogliaro, M. Bearpark, J. J. Heyd, E. Brothers, K. N. Kudin, V. N. Staroverov, T. Keith, R. Kobayashi, J. Normand, K. Raghavachari, A. Rendell, J. C. Burant, S. S. Iyengar, J. Tomasi, M. Cossi, N. Rega, J. M. Millam, M. Klene, J. E. Knox, J. B. Cross, V. Bakken, C. Adamo, J. Jaramillo, R. Gomperts, R. E. Stratmann, O. Yazyev, A. J. Austin, R. Cammi, C. Pomelli, J. W. Ochterski, R. L. Martin, K. Morokuma, V. G. Zakrzewski, G. A. Voth, P. Salvador, J. J. Dannenberg, S. Dapprich, A. D. Daniels, O. Farkas, J. B. Foresman, J. V. Ortiz, J. Cioslowski, and D. J. Fox, Gaussian, Inc., Wallingford CT, 2013.

[S2] A. Takanabe, M. Tanaka, K. Johmoto, H. Uekusa, T. Mori, H. Koshima, T. Asahi, *J. Am. Chem. Soc.,* 2016, 138, 15066-15077.

[S3] M. J. Turner, J. J. McKinnon, S. K. Wolff, D. J. Grimwood, P. R. Spackman, D. Jayatilaka and M. A. Spackman, CrystalExplorer17.5, University of Western Australia, 2017, http://hirshfeldsurface.net.